Method for Retrieving the True Backscattering Coefficient from Measurements with a Real Antenna

FAWWAZ T. ULABY, FELLOW, IEEE, CHRISTOPHER T. ALLEN, MEMBER, IEEE, AND ADRIAN K. FUNG, SENIOR MEMBER, IEEE

Abstract—Measurements made of the power backscattered by a surface at angles near normal incidence include contributions due to both coherent and incoherent scattering. Additionally, these contributions are weighted by the antenna pattern. Using a theoretical model to describe the backscattering from a rough soil surface, a procedure is developed for retrieving the true angular pattern of the backscattering coefficient σ^0 from measured estimates of σ^0, where the measured estimate is based on the usual assumption that σ^0 is approximately constant over the angular extent of the antenna beam for narrow-beam systems. The retrieved patterns of σ^0 were then used to evaluate the dependence of σ^0 on soil surface roughness at 1.5, 4.25, and 7.25 GHz.

I. Introduction

Several experimental investigations have been conducted to determine the dependence of the backscattering coefficient σ^0 on soil surface roughness, moisture content, soil type, vegetation cover, and row direction. These investigations indicate that soil surface roughness exercises the least influence on σ^0 (thereby resulting in the highest correlation between σ^0 and moisture content) when the observations are made at angles of incidence θ in the 10° to 20° range (relative to nadir).

The purpose of this paper is to analyze the observed behavior of σ^0 for nonperiodic bare soil surfaces from a theoretical standpoint. To this end, angular patterns of σ^0 measured at 1.5, 4.25, and 7.25 GHz for five surfaces with different roughness scales [1] will be used. These "measured" patterns, however, are based on measurements of the backscattered power and on the assumption that $\sigma^0(\theta)$ is approximately constant over the angular extent of the antenna beamwidth. While such an assumption may be valid for angles $\theta > 15°$, it may not always be valid for value of θ close to normal incidence. Hence, it is necessary to use the reported data to reconstruct the true angular pattern of $\sigma^0(\theta)$. This paper presents the formulation and procedure used in performing the reconstruction.

II. Scattering Model

A plane wave from air, incident upon a rough soil surface, is partly scattered into the upper hemisphere and partly transmitted into the soil medium. The part scattered into the upper hemisphere consists of two components, a coherent component reflected around the specular direction and an incoherent component scattered in all directions. In the backscattering situation, the coherent component of the backscattering coefficient σ^0_{coh} is observed only at near-nadir angles while the incoherent component, σ^0_{inc}, is present over the entire range of incidence angles θ. Thus in the general case

$$\sigma^0(\theta) = \sigma^0_{coh}(\theta) + \sigma^0_{inc}(\theta). \tag{1}$$

A. Incoherent Scattering Coefficient

The Kirchhoff (physical-optics) and the small-perturbation models [2] will be used in this study to describe the behavior of the incoherent scattering coefficient σ^0_{inc} in terms of the surface rms height σ, surface correlation function $\rho(\xi)$, and soil relative dielectric constant ϵ. For pp polarization, the expression for $\sigma^0_{inc}(\theta)$ for the Kirchoff model is given by [2]

$$\sigma^0_{inc} = 2(k|R_p(\theta)|\cos\theta)^2 \exp\{-(2k\sigma\cos\theta)^2\} \cdot \sum_{n=1}^{\infty} (4k^2\sigma^2\cos^2\theta)^n/n! \cdot \int_0^{\infty} \rho(\xi) J_0(2k\sin\theta)\,\xi\,d\xi \tag{2}$$

where $k = 2\pi/\lambda$ is the wave number, $R_p(\theta)$ is the Fresnel reflection coefficient for polarization p at incidence angle θ, and $J_0(\,)$ is the zeroth-order Bessel function. The surface correlation function is taken to have the form [3], [4]

$$\rho(\xi) = \exp[-\xi^2/(l^4 + \xi^2 L^2)^{1/2}] \tag{3a}$$

with correlation length l_c given by

$$l_c = \left[\frac{L^2}{2} + \sqrt{\left(\frac{L^2}{2}\right)^2 + l^4}\right]^{1/2} \tag{3b}$$

where l and L are small- and large-scale correlation parameters of the surface. The above form was chosen because it can accommodate surfaces with correlation functions lying between an exponential and a Gaussian function. In conjunction with radar backscattering measurements conducted for soil surfaces in 1975 [1], about 150 surface-height profiles were recorded and digitized. Four examples of surface correlation functions are shown in Fig. 1, which vary in shape between the exponential and Gaussian. This limitation, in conjunction with the

Manuscript received October 11, 1982; revised February 7, 1983. This work was supported by the National Aeronautics and Space Administration (NASA), Goddard Space Flight Center, Greenbelt, MD, under Grant NAG 5-30.

The authors are with the Remote Sensing Laboratory, University of Kansas Center for Research, Incorporated, Lawrence, KS 66045.

0196-2892/83/0700-0308$01.00 © 1983 IEEE

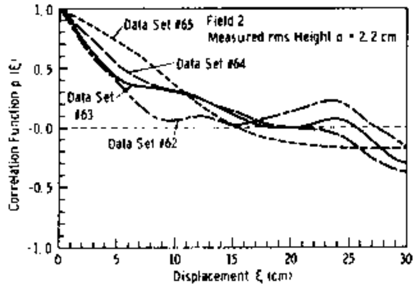

Fig. 1. Surface correlation function for each of four soil-surface profiles, each 2 m long.

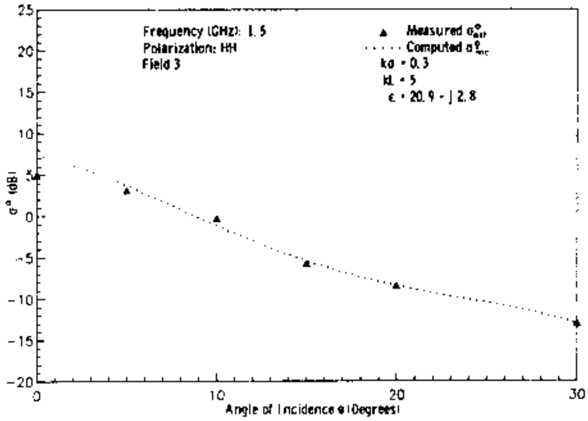

Fig. 2. Comparison of measured backscattering coefficient for a moderately rough soil surface with that computed on the basis of incoherent scattering alone and with no correction for antenna beamwidth effects.

requirements that $\rho(\xi)$ be differentiable at $\xi = 0$ and that $\rho(\xi)$ be exponential in shape for ξ slightly larger than zero, led to the use of the form given in (3a).

For convenience, only horizontally polarized data will be considered. In this case, the first-order term ($n = 1$) in (2) is identical to the first-order small perturbation model. Hence, separate expressions are not provided.

For $\theta > 10^\circ$ and relatively narrow antenna beamwidths, the coherent backscattering component σ^0_{coh} can be ignored relative to σ^0_{inc}. It was found that backscattering measurements of wet soil surfaces made under the above conditions could be modeled by (2) with good accuracy using (3) for $\rho(\xi)$ with $kl \cong 1$, and L and σ chosen appropriately. In other words, l has a minor effect on $\sigma^0_{inc}(\theta)$ in comparison to that of L. An example illustrating the fit of σ^0_{inc} to measured data is given in Fig. 2 for a medium-rough field having an rms height σ of about 1 cm. The difference between measured (estimated) σ^0 and calculated σ^0_{inc} at normal incidence is attributed to the effects of convolution by the antenna pattern. These factors are treated in Section III.

B. Coherent Scattering Coefficient

The coherent backscattering component of a rough surface is defined in terms of the surface rms height σ and the Fresnel reflection coefficient R_p, and takes the form [2]

$$\sigma^0_{coh}(\theta) = \pi k^2 |a_0|^2 \exp(-q_z^2 \sigma^2)\, \delta(q_x) \tag{4}$$

where $a_0 = 2R_p \cos\theta$, $q_x = 2k\sin\theta$, $q_z = 2k\cos\theta$, and $\delta(\,)$ is the Dirac delta function. The delta function accounts for the fact that the coherent contribution exists only at angles θ in the immediate vicinity of normal incidence. Hence, approximating $\cos\theta \cong 1$ and $\sin\theta \cong \theta$, and taking $\delta(q_z)$ to be Gaussian in shape, σ^0_{coh} can be written in the form [5]

$$\sigma^0_{coh}(\theta) = \frac{|R_p(\theta)|^2}{\beta_c^2} \exp(-4k^2\sigma^2) \exp(-\theta^2/\beta_c^2) \tag{5}$$

where β_c is an effective width of the angular pattern of σ^0_{coh}. In the present study, β_c is assumed to be a function of surface roughness and therefore is treated as a free unknown parameter to be determined from data fits, as discussed in Section IV.

The above expression leads to the same result for received power from a specular surface observed at normal incidence as does the image method (see Appendix).

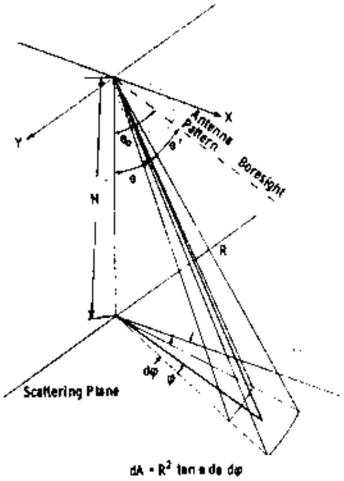

Fig. 3. Geometrical relationship between antenna and target coordinates.

III. Antenna Pattern Effects

A. Measured Estimate of σ^0

The power received due to backscattering from an area-extensive target is given by the following form of the radar equation:

$$P_r(\theta_0) = \frac{P_t \lambda^2}{(4\pi)^3} \iint (G_t(\theta,\phi) G_r(\theta,\phi) \sigma^0(\theta,\phi) R^{-4})\, dA \tag{6}$$

where P_t is the transmitted power, $G_t(\theta,\phi)$ and $G_r(\theta,\phi)$ are the transmitting and receiving antenna gains in the direction (θ,ϕ), respectively, R is the range from the radar to the differential area dA (Fig. 3), and θ_0 is the antenna boresight angle measured from nadir. The differential area dA may be expressed in terms of θ and ϕ as

$$dA = R^2 \tan\theta\, d\theta\, d\phi. \tag{7}$$

For surfaces with periodic structure, such as tillage patterns in agricultural fields, σ^0 may be a function of both θ and ϕ, but for random surfaces, σ^0 may be assumed to have no azimuthal dependence. Thus $\sigma^0 = \sigma^0(\theta)$, which is assumed to be applicable for the bare soil surfaces under consideration in this study.

TABLE I
HALF-POWER BEAMWIDTH β_e OF THE ANTENNA PRODUCT PATTERN

Frequency (GHz)	β_e
1.5	8.53°
4.25	3.01°
7.25	1.76°

The backscattering measurements used in this study were made by a truck-mounted radar spectrometer using parabolic dish antennas. The mainbeams of the measured antenna patterns were approximately Gaussian in shape and could be fitted with good accuracy to an expression of the form

$$G_t(\theta, \phi) G_r(\theta, \phi) = G_0^2 \exp(-a(\theta'/\beta_e)^2) \qquad (8)$$

where G_0^2 represents the product of the peak gains of the two antennas, $a = 2.7726$, and β_e is the effective beamwidth of the antenna pair. Table I gives the values of β_e for the three frequencies used in this study. Sidelobe contributions were ignored based on the fact that the highest sidelobe level of $G_t G_r$ was at least 30 dB below the peak value of the main lobe. Additionally, the measurement system employed range-filtering, thereby excluding any contributions from directions outside the main lobe.

In order to place the antenna pattern in the same reference frame as that of the target, a change of coordinates is necessary. Thus θ' and be expressed as [6]

$$\theta' = \cos^{-1}(\sin\theta \sin\theta_0 \cos\phi + \cos\theta \cos\theta_0) \qquad (9)$$

where θ_0 is the boresight angle measured from nadir, θ is the angle of incidence at dA, and ϕ is the azimuth angle measured from x-y projection of boresight direction (Fig. 3).

Incorporating (7)-(9) in (6) leads to

$$P_r(\theta_0) = \frac{P_t G_0^2 \lambda^2}{(4\pi)^3 R^2} \int_0^{2\pi} \int_0^{\pi/2} \exp(-a(\theta'/\beta_e{}^2) \cdot \sigma^0(\theta) \tan\theta \, d\theta \, d\phi. \qquad (10)$$

The approach usually used in experimental measurements of the backscattering coefficient is: 1) to consider only the contributions from the ground area illuminated by the projected -3-dB beamwidth pattern A_{III}, which is equivalent to limiting the integration in θ to the range corresponding to $\theta' \leqslant \beta_e/2$ and 2) to assume that $\sigma^0(\theta)$ is approximately constant over the above region of integration. These approximations lead to

$$P_r(\theta_0) = \frac{P_t G_0^2 \lambda^2 \sigma_{\text{est}}^0(\theta_0) A_{\text{III}}}{(4\pi)^3 R^4}. \qquad (11)$$

Here, the value of σ^0 that would be calculated from the above expression, and which is based on the assumption that σ^0 is constant over the antenna beamwidth, is termed the measured estimate of σ^0, or σ_{est}^0. Usually σ_{est}^0 is obtained by measuring P_r for the target area under consideration and for a calibration target of known radar cross section. Examples for $\sigma_{\text{est}}^0(\theta_0)$ are shown in Fig. 4 for soil surfaces with different rms heights.

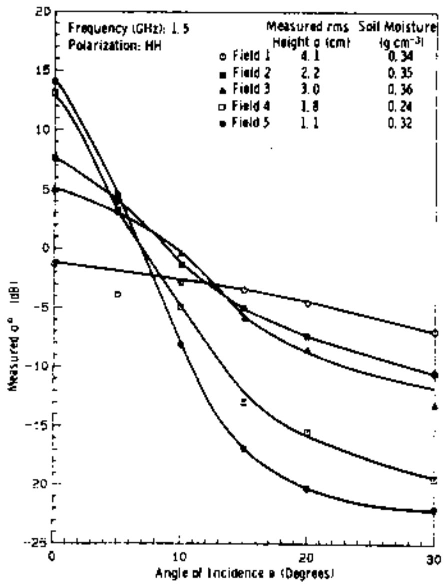

Fig. 4. Experimental observation of σ_{est}^0 for five soil surfaces with different random-roughness scales.

The relationship between σ_{est}^0 and the true $\sigma^0(\theta)$ can be obtained from (10) and (11)

$$\sigma_{\text{est}}^0(\theta_0) = \frac{R^2}{A_{\text{III}}} \int_0^{2\pi} \int_0^{\pi/2} \exp(-a(\theta'/\beta_e)^2) \cdot \sigma^0(\theta) \tan\theta \, d\theta \, d\phi. \qquad (12)$$

In practice, $\sigma_{\text{est}}^0(\theta_0)$ does indeed provide a good estimate of $\sigma^0(\theta_0)$ provided 1) the beamwidth β_e does not exceed a few degrees, 2) the surface is not very smooth, and 3) the observation angle θ_0 is not very close to normal incidence. These conditions were translated into qualitative equivalents by evaluating the error $\Delta\sigma^0(\text{dB}) = \sigma_{\text{est}}^0(\text{dB}) - \sigma^0(\text{dB})$. The evaluation was performed for a very smooth surface assumed to have a $\sigma^0(\theta)$ given by

$$\sigma^0(\theta) = 35 \exp(-\theta/2°) - 10, \quad \text{dB}. \qquad (13)$$

With the preceding expression used in (12), $\sigma_{\text{est}}^0(\theta_0)$ was computed for each of the antenna beamwidths β_e given in Table I. The results indicate that $\Delta\sigma^0 \leqslant 1$ dB if the observation angle θ_0 is beyond $\cong 2\beta_e$ from normal incidence. The hypothetical surface described by (13) is characterized by a backscattering angular pattern with a very fast decay rate. Hence, it may be concluded that the available data, which were computed on the basis of (11), can be treated as acceptable estimates of $\sigma^0(\theta_0)$ provided $\theta_0 \geqslant 2\beta_e$. This result is used in Section IV to improve the estimate of $\sigma^0(\theta_0)$ over that based on (11), for the angular region $\theta_0 < 2\beta_e$.

B. Available Data

Fig. 4 is an example of the data available to this study. Specifically, measurements of $\sigma_{\text{est}}^0(\theta_0)$ made at 1.5, 4.25, and

7.25 GHz as a function of θ_0 for $0 \leqslant \theta \leqslant 30^\circ$, are available for each of five surfaces with different surface roughness conditions. Although such measurements are available for several different soil moisture conditions, the discussion in this paper will be limited to soil surfaces with high soil-moisture contents. This choice was made to avoid the possible effects of penetration depth.

IV. Recovery of True σ^0

Based on the conclusions of Section III, A that $\sigma^0_{est}(\theta_0) \cong \sigma^0(\theta_0)$ for $\theta_0 \geqslant 2\beta_e$, the following procedure was followed for recovering $\sigma^0(\theta_0)$ for $\theta_0 < 2\beta_e$:

1) Since the contribution of the coherent term σ^0_{coh} to the total σ^0 is limited to angles θ_0 that are in the immediate vicinity of normal incidence, it can be neglected in the region $\theta_0 > 2\beta_e$. Hence, in this region, $\sigma^0(\theta_0) \cong \sigma^0_{inc}(\theta)$.

2) For each surface and frequency combination, the expression given by (2) is made to fit the available $\sigma^0_{est}(\theta_0)$ data over the region $\theta_0 > 2\beta_e$. The Fresnel reflection coefficient is computed from dielectric-constant values based on dielectric-constant values based on dielectric-constant measurements given as a function of moisture content by Wang and Schmugge [7] for a soil of similar textural composition to the soil under consideration. In generating the fit, the rms height σ and surface correlation length l_e were treated as free parameters. The best-fit value of σ was found to be within a factor of 2 of that measured from a relatively short, one-dimensional profile of the surface.

Examples of these fits are shown in Fig. 5. The solid curves are based on fitting (2) to the measured points for $\theta_0 \geqslant 15^\circ$, but are drawn for the entire 0-to-30° range to illustrate the magnitude of the error between σ^0_{est} and σ^0_{inc}. For the rough surface (Field 1) with a measured σ of 4.3 cm, $\sigma^0_{est}(\theta_0) \cong \sigma^0_{inc}(\theta_0)$ at all angles, with the maximum difference being about 1 dB at $\theta_0 = 0$. In contrast, for the smooth surface of Field 5 with a measured σ of 1.1 cm, σ^0_{inc} is completely inadequate for $\theta_0 < 15^\circ$, which is due to ignoring the contribution of σ^0_{coh} and antenna-pattern effects.

3) For a case such as that shown in Fig. 5(b), the fit of $\sigma^0_{inc}(\theta_0)$ to $\sigma^0_{est}(\theta_0)$ for $\theta_0 > 15^\circ$ provides estimates of σ and L for that surface. With σ known, a more exact expression for σ^0 can now be written by including in (1) both σ^0_{coh} and σ^0_{inc} as given by (2) and (5). The only unknown quantity is β_c, the effective width of the coherent backscattering pattern. This quantity is determined by finding the best fit between measured $\sigma^0_{est}(\theta_0)$ and calculated $\sigma^0_{est}(\theta_0)$ on the basis of (12) with $\sigma^0(\theta)$ on the right-hand side of (12) being the sum of (2) and (5). An example of this process is shown in Fig. 6. The figure includes curves for 1) $\sigma^0_{inc}(\theta_0)$, 2) $\sigma^0_{coh}(\theta_0)$, 3) $\sigma^0(\theta) = \sigma^0_{coh}(\theta) + \sigma^0_{inc}(\theta)$, and points for 1) measured $\sigma^0_{est}(\theta_0)$ and 2) calculated $\sigma^0_{est}(\theta_0)$. The agreement between the two sets of points is observed to be quite good.

4) Based on the above procedure, the "true" $\sigma^0(\theta_0)$ curves were generated for all the surfaces and for each of the three microwave frequencies. Fig. 7(a)–(f) shows plots of $\sigma^0(\theta_0)$ and of the measured $\sigma^0_{est}(\theta_0)$ for Field 3 (slightly rough) and

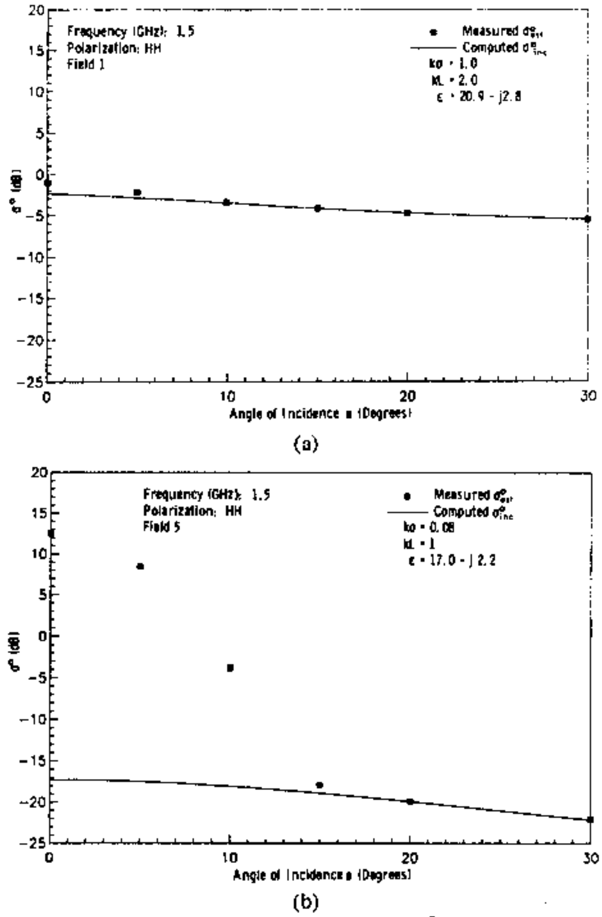

Fig. 5. Ignoring the coherent component of σ^0 and not accounting for antenna beamwidth effects results in negligible errors for a rough surface (a), but not for a smooth surface (b).

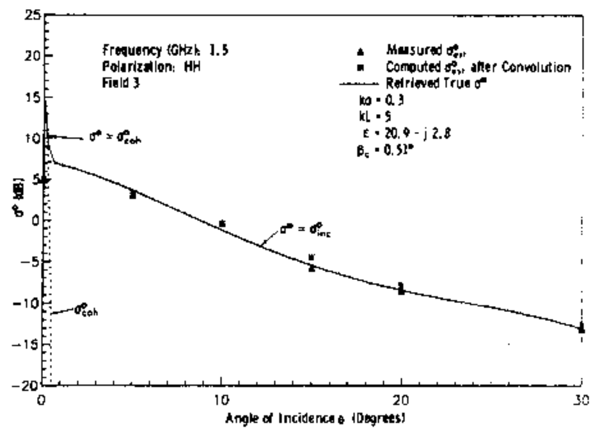

Fig. 6. Comparison of measured σ^0_{est} with computed σ^0_{est} for a moderately rough soil surface.

Field 5 (smooth). The results for Field 1 (roughest field) indicate a negligible difference between σ^0 and σ^0_{est}; those for Field 2 show a difference of as much as 5 dB at 1.5 GHz for $\theta = 0^\circ$ and 5° and smaller differences at 4.25 and 7.25 GHz; and those for Field 4 are intermediate between the results shown in Fig. 7 for Fields 3 and 5. Details of the above procedure and the results obtained are given in [8].

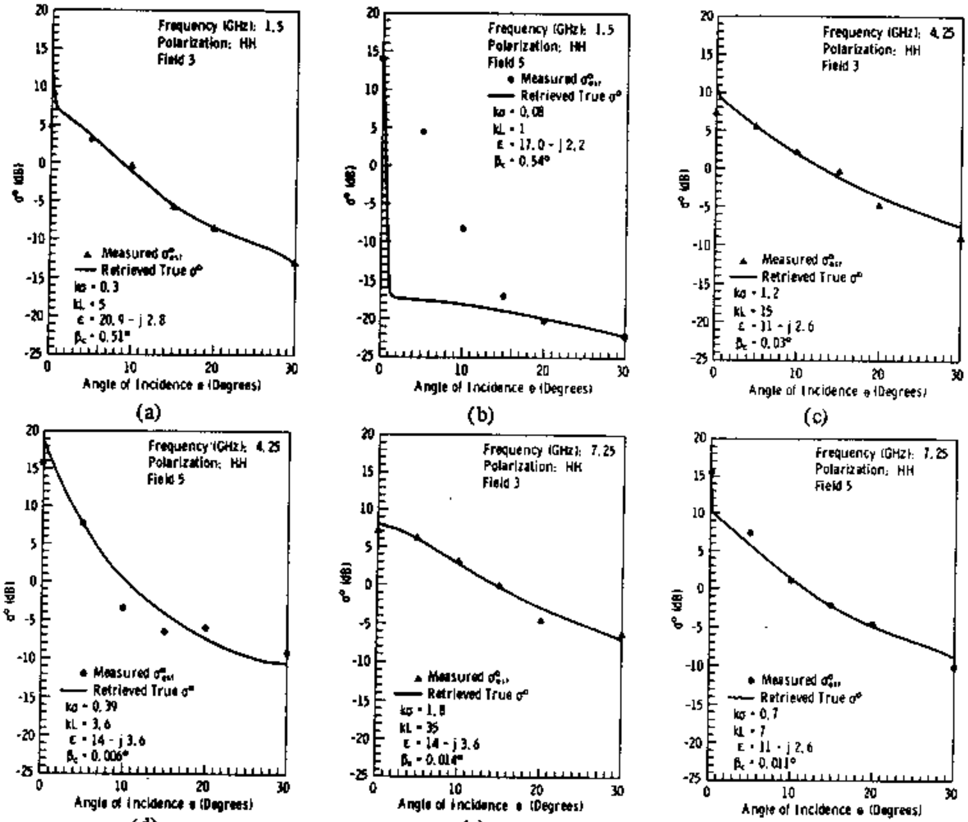

Fig. 7. Comparison of measured and true σ^0 for a moderately rough (Field 3) and a smooth surface (Field 5) at 1.5, 4.25, and 7.25 GHz.

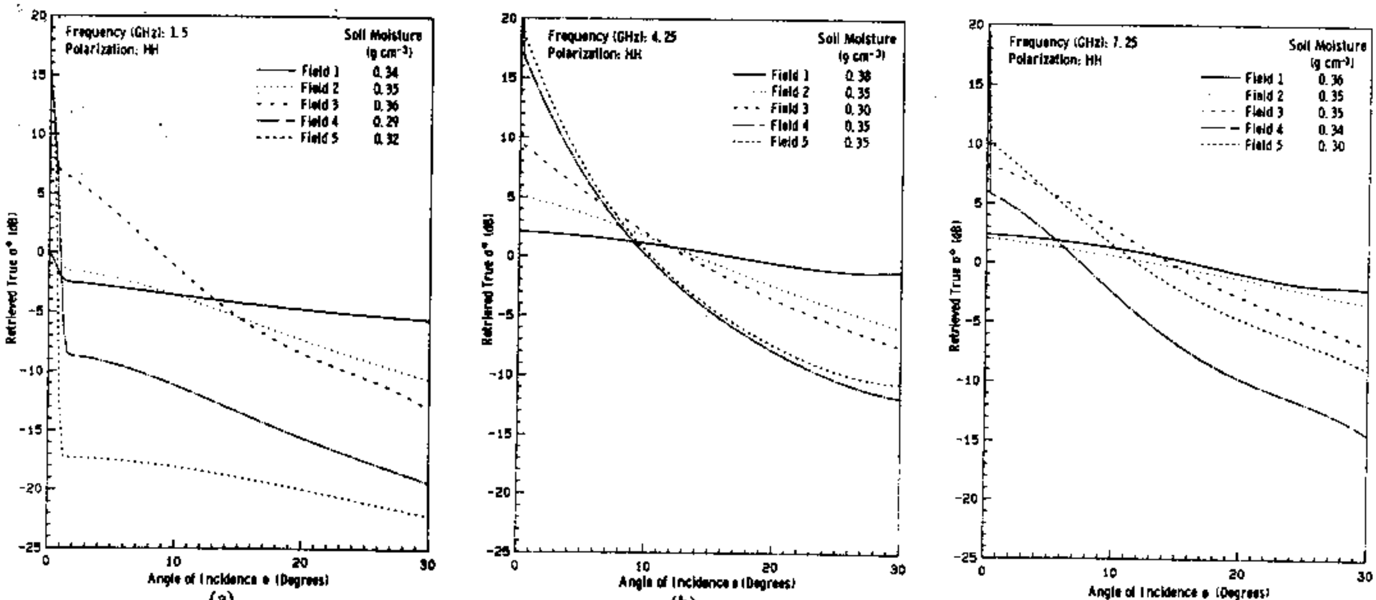

Fig. 8. Angular pattern of retrieved true σ^0 for five soil surfaces with different roughness scales at (a) 1.5 GHz, (b) 4.25 GHz, and (c) 7.25 GHz.

V. σ^0 Dependence on Surface Roughness

One of the main objectives of this paper is to evaluate the dependence of σ^0 on soil surface roughness. Performing such an evaluation on the basis of the theoretical models above would require *a priori* knowledge of 1) the ranges of values that the rms height σ and surface correlation length l_e take for soil surfaces under natural conditions, and 2) any relationships that may exist between σ, l_e, and the soil moisture content m_v, again for surfaces under natural conditions. In the absence of this information, the approach taken here is to evaluate the dependence on surface roughness using the "true" $\sigma^0(\theta)$ curves derived in the previous section by effectively removing the convolution effects of the antenna pattern.

Fig. 8 shows plots of the retrieved $\sigma^0(\theta)$ for the five fields at 1.5, 4.25, and 7.25 GHz. It is observed that the vertical spread in the magnitude of σ^0 (due to differences in surface roughness) is smallest at 4.25 GHz in the angular range around $\theta = 10^\circ$. This result is in good agreement with ground-based and airborne observations [2], [9], [10].

VI. Conclusions

This paper has shown how a theoretical backscattering model can be used in conjunction with σ^0 versus θ measurements (made with a finite-beam antenna) to retrieve the true angular pattern of σ^0, even though the statistical roughness parameters of the surface were unknown. The patterns so retrieved support experimental observations indicating that σ^0 has a weak dependence on surface roughness at 4.25 GHz for θ around 10°.

Appendix

For a specular surface with rms height $\sigma = 0$, the coherent component of σ^0, σ^0_{inc} defined by (5), should lead to the same expression for received power at normal incidence as one would obtain using the image method. In the image method, the transmitting antenna "sees" its image in the reflection and hence may be modeled as two antennas with the same gain G_0 and separated by a distance $2h$, where h is the height of the antenna above the surface. The received power in this image case is given by

$$P_r = \frac{P_t G_0^2 \lambda^2 \, |R_p|^2}{(4\pi)^2 (2h)^2} \tag{A1}$$

where R_p is the Fresnel reflection coefficient.

In terms of the scattering coefficient σ^0, the received power is given by the radar equation, from (6), as

$$P_r = \frac{P_t \lambda^2}{(4\pi)^3} \iint \frac{G^2 \sigma^0}{R^4} \, dA. \tag{A2}$$

For a specular surface with rms height $\sigma = 0$ and surface correlation length $L = \infty$, $\sigma^0_{\text{inc}} = 0$ and σ^0_{coh} is given from (5) by

$$\sigma^0_{\text{coh}}(\theta) = \frac{|R_p(\theta)|^2}{{\beta_c}^2} \exp(-\theta^2/\beta_c^2) \tag{A3}$$

where β_c is the effective beamwidth of σ^0_{coh}. The magnitude of β_c is of the order of 1° or smaller. Hence the contribution of $\sigma^0_{\text{coh}}(\theta)$ to the integral of (A2) becomes insignificant for θ beyond a few degrees, in which case the quantity dA/R^4 may be approximated as follows:

$$\frac{dA}{R^4} = \frac{\cos\theta \sin\theta}{h^2} \, d\theta \, d\phi \cong \frac{1}{h^2} \, \theta d\theta d\phi \tag{A4}$$

by setting $\sin\theta \cong \theta$ and $\cos\theta \cong 1$. With the antenna gain G being approximately constant and equal to G_0 over the effective region of integration in (A2) inserting (A3) and (A4) in (A2) and integrating leads to

$$P_r = \frac{P_t G_0^2 \lambda^2}{(4\pi)^3} \frac{|R_p|^2}{(2h)^2}, \tag{A5}$$

which is identical to the image-method expression given by (A1).

References

[1] F. T. Ulaby, P. P. Batlivala, and M. C. Dobson, "Microwave backscatter dependence on surface roughness, soil moisture, and soil texture, part I: Bare soil," *IEEE Trans. Geosci. Elec.*, vol. GE-16, no. 4, pp. 286–295, 1978.

[2] F. T. Ulaby, R. K. Moore, and A. K. Fung, *Microwave Remote Sensing: Active and Passive, Vol. II: Radar Remote Sensing and Surface Scattering and Emission Theory*, ch. 12. Reading, MA: Addison-Wesley, 1982.

[3] F. T. Ulaby, K. Kouyate, and A. K. Fung, "A backscattering model for a randomly perturbed surface," Univ. of Kansas Center for Res., Inc., Lawrence, RSL Tech. Rep. 460-4, 1981.

[4] A. K. Fung and H. J. Eom, "An approximate model for backscattering and emission from land and sea," Univ. of Kansas Center for Res., Inc., Lawrence, RSL Tech. Rep. 460-5, 1982.

[5] ——, "Coherent scattering of a spherical wave from an irregular surface," Univ. of Kansas Center for Res., Inc., Lawrence, Rep. 485-3, 1982.

[6] R. M. Axline, Jr., and A. K. Fung, "Experimental and simulated study of scattering from randomly rough surfaces," Univ. of Kansas Center for Res., Inc., Lawrence, RSL Tech. Rep. 222-2, 1974.

[7] J. R. Wang and T. J. Schmugge, "An empirical model for the complex dielectric permittivity of soils as a function of water content," NASA Tech. Memo. 79659, 1978.

[8] C. T. Allen, F. T. Ulaby, and A. K. Fung, "A model for the radar backscattering coefficient of bare soil," Univ. of Kansas Center for Res., Inc., Lawrence, RSL Tech. Rep. 460-8, 1982.

[9] G. A. Bradley and F. T. Ulaby, "Aircraft radar response to soil moisture," *Remote Sensing Environ.*, vol. 11, pp. 419–438, 1981.

[10] T. J. Jackson and T. J. Schmugge, "Aircraft active microwave measurements for estimating soil moisture," *Photogrammetr. Eng.*, vol. 47, pp. 801–805, 1981.

Fawwaz T. Ulaby (M'68–SM'74–F'80), for a photograph and biography, please see page 238 of this issue of this Transactions.

Christopher T. Allen (M'78) was born in Independence, MO, on October 7, 1958. He received the B.S. and M.S. degrees from the University of Kansas, Lawrence, in 1980 and 1981, respectively. He is currently working towards the Ph.D. degree in electrical engineering.

He has been with the Remote Sensing Laboratory at the University of Kansas since 1980 and has participated in research into the microwave backscattering properties of soil surfaces and vegetation canopies. He is currently a Graduate Research Assistant and is involved in modeling the response of vegetation to radar.

Mr. Allen is a member of Eta Kappa Nu and Tau Beta Pi.

Adrian K. Fung (S'60–M'66–SM'70), for a photograph and biography, please see page 270 of this issue of this Transactions.